

MUSON: A Reasoning-oriented Multimodal Dataset for Socially Compliant Navigation in Urban Environments

Zhuonan Liu¹, Xinyu Zhang¹, Zishuo Wang¹, Tomohito Kawabata¹, Xuesu Xiao², Ling Xiao^{1,†} *Senior Member, IEEE*

Abstract—Socially compliant navigation requires structured reasoning over dynamic pedestrians and physical constraints to ensure safe and interpretable decisions. However, existing social navigation datasets often lack explicit reasoning supervision and exhibit highly long-tailed action distributions, limiting models’ ability to learn safety-critical behaviors. To address these issues, we introduce MUSON, a multimodal dataset for short-horizon social navigation collected across diverse indoor and outdoor campus scenes. MUSON adopts a structured five-step Chain-of-Thought annotation consisting of perception, prediction, reasoning, action, and explanation, with explicit modeling of static physical constraints and a rationally balanced discrete action space. Compared to SNEI, MUSON provides consistent reasoning, action, and explanation. Benchmarking multiple state-of-the-art Small Vision Language Models on MUSON shows that Qwen2.5-VL-3B achieves the highest decision accuracy of 0.8625, demonstrating that MUSON serves as an effective and reusable benchmark for socially compliant navigation. The dataset is publicly available at <https://huggingface.co/datasets/MARSLab/MUSON>.

Index Terms—Socially compliant navigation, Multimodal dataset, Chain-of-thought annotation, Multimodal small language models

I. INTRODUCTION

RESEARCH in embodied navigation has traditionally focused on long-horizon, target-oriented tasks, as exemplified by benchmarks such as R2R [1] and RxR [2]. These benchmarks primarily address the global planning question of “where to navigate,” emphasizing destination reaching over local decision-making. While effective for long-range navigation, such paradigms are insufficient for scenarios that require fine-grained interaction with humans.

In contrast, socially compliant navigation emphasizes “how to navigate” within human-centered environments, where agents must make precise, short-horizon decisions under dynamic social constraints. This setting demands not only spatial awareness but also the ability to reason about pedestrian behaviors, shared spaces, and social norms. As a result, conventional navigation models trained on long-horizon trajectory datasets are ill-suited for social navigation tasks.

Recent efforts have begun to explore learning-based approaches for social navigation, including the use of vision language models (VLMs) to infer socially appropriate actions [3]–[5]. For these approaches to be effective, however,

high-quality data with explicit reasoning and action supervision is essential. In particular, models must be trained with consistent Chain-of-Thought (CoT) annotations and standardized action instructions to learn socially normative behaviors and ensure safety in crowded or interactive environments.

Although some socially oriented navigation datasets, such as SNEI [6], have been proposed, they suffer from several critical limitations: (1) limited scale, containing only 325 five-turn conversations; (2) highly long-tailed action distributions, with *move forward* and *stop* accounting for approximately 78.46% of all actions; and (3) severe inconsistencies across reasoning, actions, and explanations. These issues substantially hinder the learning of robust and socially compliant decision-making policies.

To address these challenges, we propose MUSON, a reasoning-oriented social navigation dataset designed to support socially compliant navigation with VLMs. MUSON integrates high-quality annotations of both dynamic and static environmental constraints, balanced and standardized action distributions, and diverse multi-scene data. By fine-tuning on MUSON, VLMs can acquire structured reasoning and robust action inference capabilities. Experimental results demonstrate that, when trained on MUSON, even small-scale VLMs can achieve strong decision-making performance aligned with social norms.

The contributions of this work are summarized as follows:

- **A reasoning-oriented social navigation dataset.** We introduce MUSON, a multimodal dataset for short-horizon, socially compliant navigation, consisting of 800 curated egocentric samples annotated with a five-step CoT pipeline and explicit modeling of dynamic and static constraints.
- **A principled action and annotation design for social navigation.** MUSON discretizes continuous commands into six language-aligned action categories and adopts physics-aware, geometrically balanced curation to alleviate long-tailed action bias while preserving rare but safety-critical interactive behaviors.
- **Benchmark baselines and evaluation protocol.** We benchmark four state-of-the-art Small Vision Language Models (SVLMs) on MUSON using a multidimensional evaluation protocol that measures safety, long-tail reliability, and reasoning consistency. Results show that Qwen2.5-VL-3B achieves the highest decision accuracy of 0.8625, demonstrating that MUSON is an effective and reusable benchmark for socially compliant navigation.

[†]Corresponding author: ling@ist.hokudai.ac.jp.

This work was supported by JSPS KAKENHI (Grant No. 24K20787).

¹Graduate School of Information Science and Technology, Hokkaido University, Sapporo, Japan.

²Graduate School of Computer Science, George Mason University, Fairfax County, Virginia, USA

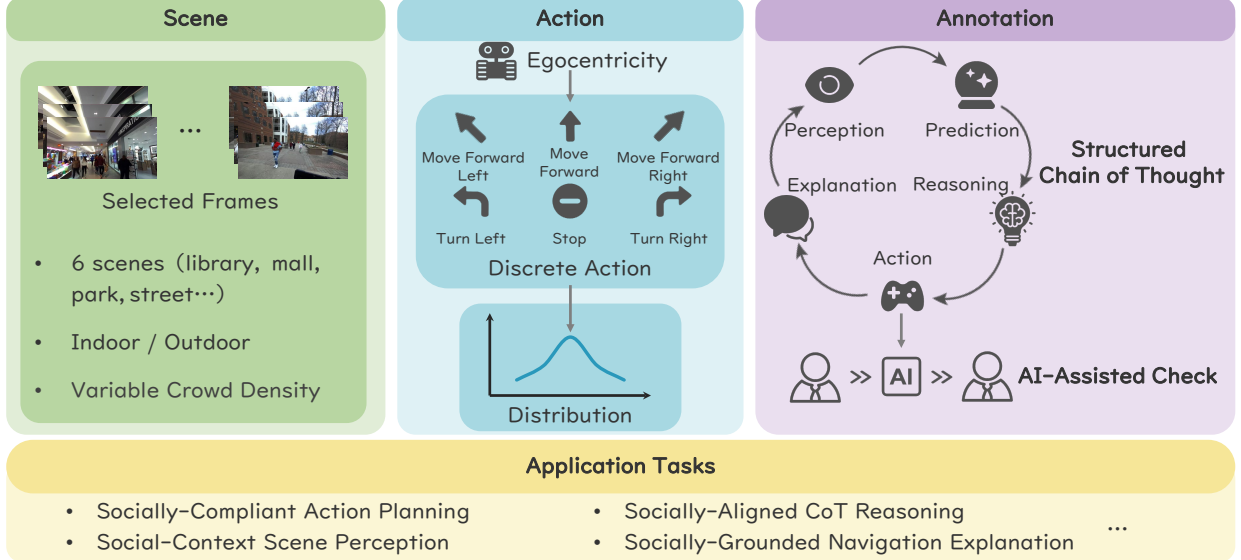


Fig. 1. **The MUSON dataset construction pipeline.** MUSON covers diverse real-world scenes across indoor and outdoor environments with varying crowd densities. Continuous navigation behaviors are discretized into six egocentric action categories with a rational distribution that preserves safety-critical corner cases to mitigate long-tail issues. Each sample is annotated using a structured five-step CoT, followed by a Human–AI–Human verification process to ensure annotation consistency and quality. MUSON supports multiple downstream tasks, including socially-compliant action planning, socially-aligned CoT reasoning, social-context scene perception, and socially-grounded navigation explanation.

II. RELATED WORK

A. Short-Horizon Social Navigation

Robot navigation research can be broadly categorized into long-horizon and short-horizon paradigms. Representative works such as R2R [1], RxR [2], and VLN-CE [7] have established long-horizon instruction following as the dominant setting in vision language navigation. These datasets focus on enabling agents to understand complex natural language instructions and leverage topological memory of maps and global planning to reach distant goals [8], [9]. As a result, they often assume that low-level controllers have already solved local obstacle avoidance and physical interactions, abstracting away short-term safety and social compliance. But the actual situation is far more complex than imagined, and agents must make socially compliant policy with interactive awareness based on local and dynamic observations [10]. Consequently, mastering *short-horizon navigation* emerges as a fundamental prerequisite. Within this setting, the SNEI [6] dataset represents a representative effort that leverages natural language to bridge perception and socially compliant behavior. Built upon the SCAND [11] dataset, SNEI introduces multi-dimensional annotations covering perception, prediction, reasoning, action, and explanation, enabling VLMs to learn human-like social reasoning in dynamic environments.

However, SNEI suffers from three key limitations. First, it is small in scale, containing only 325 five-turn conversations, which is insufficient for effectively tuning VLMs. Second, its action annotations are highly long-tailed, with dominant actions such as move forward overwhelmingly represented, limiting coverage of rare but safety-critical social behaviors. Third, it exhibits severe inconsistencies across reasoning, actions, and explanations, hindering models from learning

structured and generalizable decision logic. This paper aims to address the above-mentioned issues.

B. VLMs for Action Selection

Translating the semantic understanding capabilities of VLMs into precise control signals is a core challenge in embodied intelligence. Early approaches predominantly adopted end-to-end imitation learning, utilizing CNNs or recurrent neural networks (RNNs) to map raw pixels directly to actions [12], [13]. While efficient, these methods suffer from a “black-box” nature, lacking the causal reasoning required to generalize across unseen scenes [14]. Recently, the paradigm has shifted towards VLMs, such as PaLM-E [15] and RT-2 [16], which leverage vast parameters for open-ended planning and reasoning [17]–[19]. Despite their strong generalization, large-scale VLMs face significant hurdles in real-world deployment: their prohibitive computational overhead and high inference latency obstruct real-time closed-loop control, while their open-ended generation mechanism poses risks of hallucination and safety violations [20], [21].

To reconcile high-level reasoning with deployment efficiency [22], research focus is turning toward small-scale VLMs and lightweight architectures [23]–[27]. Simultaneously, CoT prompting has proven effective in eliciting reasoning capabilities in language models [28]. However, effectively synergizing lightweight architectures with CoT to achieve safety-critical, reasoning-aware navigation remains an underexplored area. Moreover, existing lightweight approaches often struggle to balance the depth of reasoning with the determinacy of control. This paper investigates the potential of enabling lightweight models to master complex embodied decision-making through alignment with high-quality, structured reasoning data.

III. THE MUSON DATASET

A. Data Collection and Scene

Data Source and Diversity. Fig. 1 shows the MUSON dataset construction pipeline. MUSON is derived from the real-world first-person perspective dataset, MuSoHu [29]. To capture the complexity of urban environments, we curate 800 frames covering diverse and safety-critical scenarios. The dataset spans a wide range of indoor and outdoor settings, including libraries, malls, plazas, and streets, with crowd densities ranging from sparse to dense. This diversity supports robust model adaptation to real-world navigation conditions.

Local Decision-Making. Unlike long-horizon navigation tasks that emphasize where to navigate, MUSON focuses on how to navigate within the immediate environment. By removing dependence on long-term goals or instruction history, the dataset isolates single-frame decision making and encourages models to prioritize immediate safety and social compliance in each local scene.

Ego-centric Reference Frame. To match the first-person nature of embodied perception, we adopt a strictly ego-centric reference frame in MUSON. All spatial descriptions are expressed using relative directions (e.g., front, front-left) anchored to the camera coordinate system, rather than absolute world coordinates. This design avoids viewpoint- and scene-specific ambiguities, improves cross-scene transferability, and ensures consistent geometric alignment between language and visual observations, facilitating robust spatial reasoning.

B. Action Definition and Distribution

To align with the token generation mechanism of VLMs, we discretize continuous trajectories into six distinct semantic actions. This transformation into discrete action selection offers two primary advantages: 1) Compared to continuous regression, selecting actions from a finite semantic set simplifies the prediction target, allowing the model to focus on high-level decision intentions rather than precise metric estimation. 2) Discrete tokens align naturally with CoT texts, positioning the action as the logical conclusion of the reasoning process.

In addition, to address the long-tailed distribution and positional bias in navigation data, we adopted a targeted curation strategy to construct a distribution that balances physical priors with geometric symmetry. The statistics are shown in Table I.

Physically Grounded Action Balancing. Given that “move forward” is a high-frequency action in navigation, we retained approximately 56.6% of “move forward” samples. This aligns with real-world physical laws, endowing the model with necessary forward momentum and preventing overly conservative decision-making in safe scenarios due to excessive balancing.

Geometric Symmetry. To eliminate *Positional Bias* where models tend to turn towards a specific side, we strictly controlled the quantity of samples for left and right directions to be equivalent:

- **Oblique Motion:** *Move Forward Left* and *Move Forward Right* both have 118 samples.
- **Turning:** *Turn Left* and *Turn Right* both have 32 samples.

This geometric balance forces the model to make decisions based on environmental features rather than statistical priors.

TABLE I
ACTION DISTRIBUTION STATISTICS IN MUSON

Action Category	Count	Percentage
Move Forward	453	56.6%
Forward Left	118	14.75%
Forward Right	118	14.75%
Stop	47	5.9%
Turn Left	32	4.0%
Turn Right	32	4.0%
Total	800	100%

Preserving Safety-Critical Corner Cases. Although *Stop* (5.9%) and *Turn Left* or *Turn Right* (4.0% each) belong to long-tailed classes, our curation ensures they cover critical high-risk scenarios such as dead ends and sudden pedestrian crossings, guaranteeing the model’s ability to learn from corner cases.

C. Annotation Schema

The 5-Step CoT. To mitigate the “black box” opacity of end-to-end navigation, MUSON establishes a structured annotation schema containing a 5-Step CoT, compels the model to execute a complete logical deduction loop before outputting an action.

- 1) **Perception:** Fine-grained identification of dynamic entities and static constraints within the field of view that may influence navigation, including visual attributes and ego-centric spatial relationships.
- 2) **Prediction:** Forecasting future object states. Static objects are labeled as stationary, while trajectories of dynamic objects are predicted to assess potential collision risks.
- 3) **Reasoning:** A critical bridge between perception and action, where social norms and physical constraints are jointly considered to derive policy-level decisions.
- 4) **Action:** Selecting an optimal decision from a discrete action space based on the reasoning outcome.
- 5) **Explanation:** A first-person retrospective justification that summarizes the preceding chain of thought and explains the selected action.

AI-Assisted Quality Control. To ensure high annotation fidelity, we adopt a rigorous *Human-AI-Human* verification pipeline consisting of three stages:

- 1) **Initial Annotation.** Two human annotators independently annotate each sample across perception, prediction, reasoning, action, and explanation.
- 2) **AI-Assisted Audit.** We employ a TinyLLaVA model trained on MUSON to perform automated logical consistency checks. Samples in which the model’s inferred reasoning or decisions substantially deviate from human annotations are flagged for further review.
- 3) **Final Arbitration.** A senior expert conducts a comprehensive review of all flagged samples, including both inter-annotator disagreements and human–AI inconsistencies, to determine the final ground truth (GT) annotations.

D. Evaluation Tasks

Based on the structured annotation schema and diverse scenarios of MUSON, we formulate four distinct tasks to eval-

uate the multidimensional capabilities of navigation agents. These tasks progress from fundamental perception to complex reasoning and decision-making.

Socially-Compliant Action Planning. This task serves as the core control evaluation, assessing the agent’s ability to make safe and normative decisions. Given an ego-centric visual observation, the model must predict the optimal action token $a \in \mathcal{A}$ from the six discrete semantic actions defined in Section III-B. Unlike standard obstacle avoidance, this task emphasizes *social compliance*, where the agent must respect social norms (e.g., yielding to pedestrians, maintaining distance) implicitly embedded in the dataset.

Social-Context Scene Perception. This task evaluates the *Perception* and *Prediction* components of the 5-step schema. The model is required to generate fine-grained text descriptions of the environment. Crucially, these descriptions must strictly adhere to the ego-centric reference frame, accurately identifying static constraints and dynamic agents using relative directional terms (e.g., “front-left”, “bearing”).

Socially-Aligned CoT Reasoning. This task targets the *Reasoning* step, acting as the bridge between perception and action. The model must generate a logical chain that weighs observed environmental factors against social norms to derive a policy recommendation. This evaluates whether the model understands the *why* behind a navigation scenario, rather than just fitting visual patterns to action labels.

Socially-Grounded Navigation Explanation. Addressing the “black box” issue, this task corresponds to the final “Explanation” step. The model must provide a retrospective natural language justification for its chosen action. Unlike the intermediate reasoning process, this explanation is user-facing, requiring the model to summarize the decision logic in a concise, human-understandable format.

E. Comparison with SNEI.

While SNEI represents an early attempt to incorporate explanatory text into social navigation, it remains limited as a training benchmark. MUSON is designed to explicitly address these limitations (as shown in Fig. 2):

1) **Scale and Coverage.** SNEI contains only 325 five-turn conversations, which is insufficient for effectively tuning vision language models. In contrast, MUSON expands the dataset to 800 curated samples, covering a broader range of dynamic and static navigation scenarios.

2) **Action Distribution.** SNEI exhibits a highly long-tailed action distribution, with dominant actions overwhelming rare but safety-critical behaviors. MUSON adopts a balanced and standardized discrete action space, improving coverage of diverse social interactions and decision outcomes.

3) **Reasoning Consistency.** Although SNEI provides explanatory text, it lacks structured intermediate supervision, resulting in frequent inconsistencies across reasoning, actions, and explanations. MUSON enforces a structured five-step CoT annotation, ensuring logical consistency throughout perception, reasoning, action selection, and explanation.

IV. EVALUATION AND METRICS

A. Safety and Social Compliance

Motivated by safety metrics commonly adopted in low-level motion planning, we introduce collision rate (CR) as the primary safety metric for high-level decision making. In embodied navigation, the cost of decision errors is highly asymmetric [30]: unsafe decisions may lead to collisions with severe consequences, whereas overly conservative actions typically incur only minor efficiency loss. Accordingly, CR captures this asymmetric risk profile via an asymmetric penalty mechanism, rather than treating all errors equally as in conventional classification accuracy.

$$CR = \frac{1}{N} \sum_{i=1}^N \mathbb{I}(a_{pred}^i \in \mathcal{A}_{go} \cap a_{gt}^i \in \mathcal{A}_{stop}), \quad (1)$$

where N denotes the total number of samples in the evaluation set, $\mathbb{I}(\cdot)$ denotes the indicator function, a_{pred}^i denotes i -th predicted result of the model, a_{gt}^i represents i -th ground truth of the model, \mathcal{A}_{go} represents aggressive actions (e.g., move forward, forward left, and forward right), and \mathcal{A}_{stop} represents avoidance actions (e.g., stop, turn left, and turn right).

This metric differentiates between two types of errors to enforce safety: 1) Aggressive Errors: Occur when the ground truth requires avoidance but the model chooses to force through. These are penalized as collisions. 2) Conservative Errors: Occur when the ground truth allows passage but the model chooses to stop or turn. A lower CR value indicates more robust defensive decision-making in hazardous scenarios.

B. Concept Understanding and Reasoning Logic

Based on the “*Navigation as Semantics*” hypothesis, we posit that decisions stem from reasoning about environmental causality. Since n-gram-based metrics such as BLEU [31] fail to capture logical and semantic consistency, we adopt the SBERTScore [32] as a proxy metric for evaluating reasoning quality. Specifically, we use a pre-trained SBERT encoder to embed both predicted and reference texts into a shared high-dimensional semantic space, and compute their similarity using cosine similarity:

$$S_{bert} = \frac{E(T_{pred}) \cdot E(T_{gt})}{\|E(T_{pred})\| \|E(T_{gt})\|}, \quad (2)$$

where T_{pred} denotes the explanation text generated by the model, T_{gt} denotes the ground truth annotation provided by human experts, and $E(\cdot)$ represents the semantic embedding vector output by the SBERT encoder.

A high SBERTScore indicates that the model’s generated CoT is semantically aligned with expert-provided reasoning. This suggests that the model captures meaningful physical and social cues underlying navigation decisions, rather than relying solely on surface-level action patterns.

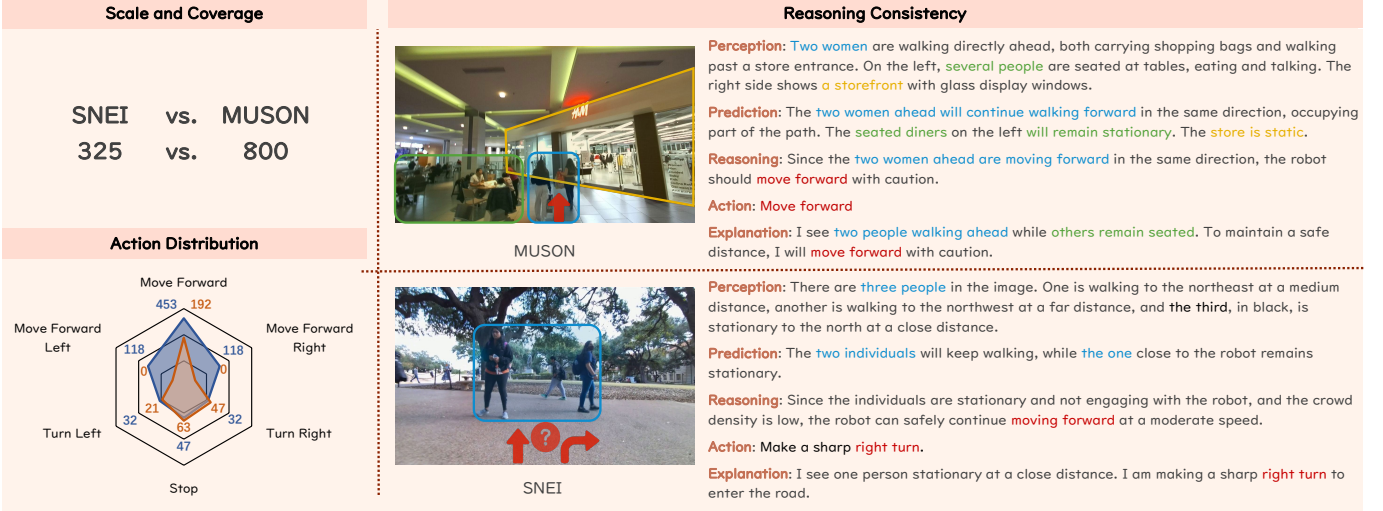


Fig. 2. Visualization comparisons of samples from SNEI and MUSON.

C. Decision Accuracy and Fairness

Accuracy: This metric measures the prediction correctness across all samples, which is calculated as:

$$\text{Accuracy} = \frac{1}{N} \sum_{i=1}^N \mathbb{I}(a_{pred}^i = a_{gt}^i), \quad (3)$$

Macro-averaged F1 Score: Given the long-tailed distribution of navigation data (dominated by move forward), the above-mentioned accuracy metric (Eq. 3) tends to mask model failures on sparse classes. Following R2R, we employ Macro-F1 to assign equal weight to sparse actions (e.g., stop/turn left) and dominant actions:

$$\text{Macro-F1} = \frac{1}{|C|} \sum_{c \in C} \frac{2 \times P_c \times R_c}{P_c + R_c}, \quad (4)$$

where $|C|$ is the number of action classes. P_c is the precision for class c . R_c is the recall for class c .

This ensures that the model’s ability to handle low-frequency but high-value critical scenarios is fairly evaluated, validating its robustness under long-tailed distributions.

V. EXPERIMENTS AND ANALYSIS

In this section, we benchmark representative SVLMs on the proposed MUSON dataset to evaluate their embodied reasoning capabilities. We first introduce the baseline models and fine-tuning protocols, and then conduct a unified evaluation of safety, reasoning quality, and long-tail decision-making performance.

A. Experimental Setup

Base Model Selection. To evaluate the generality and model-agnostic applicability of MUSON across different architectural paradigms, we benchmark four representative SVLMs with comparable parameter scales (below 3B). These models embody diverse architectural design choices, enabling a controlled evaluation of whether MUSON consistently benefits

SVLMs with different inductive biases. *TinyLLaVA* [25] (*Phi-2-based*): A dense, ultra-lightweight SVLM used to probe the lower bound of parameter efficiency. *NVILA* [33]: An SVLM emphasizing enhanced cross-modal interaction, evaluating the impact of multimodal fusion quality on navigation performance. *Qwen2.5-VL-3B* [34]: A strong instruction-following SVLM serving as a high-performance baseline. *MoE-LLaVA* [26]: An MoE-based SVLM with sparse activation, assessing the benefits of expert specialization under constrained computation.

Structured Prompting & SFT Strategies. To overcome the issue of logical forgetting often seen in small models during complex tasks, we designed an explicit injection paradigm:

1) *Prompt Engineering.* Via the System Prompt, we establish the agent’s identity as a “Safety Expert.” We inject MUSON’s three core priors: physical feasibility, social compliance, and safety first, as inviolable decision boundaries. Simultaneously, we enforce the model to follow the 5-Step CoT format, compelling it to explicitly parse environmental causality before generating action tokens.

2) *Training Strategy.* We employ Full-Parameter Supervised Fine-Tuning (SFT), optimizing both the LLM and connector parameters based on a causal language modeling objective. To accelerate convergence and retain general visual features, the model is initialized from pre-trained multimodal weights. The vision tower remains frozen throughout the fine-tuning process, effectively transforming the implicit experience of human experts into explicit reasoning capabilities. Fig. 3 shows stable fine-tuning dynamics on MUSON, with steadily decreasing loss and a gradually diminishing gradient norm, indicating smooth and stable convergence.

Implementation Details. All experiments were conducted using the PyTorch framework with DeepSpeed ZeRO-3 optimization. Training was performed on 8 NVIDIA RTX 8000 GPUs. We employ the AdamW optimizer with a cosine learning rate schedule, setting the initial learning rate to 2×10^{-5} and a warmup ratio of 0.03. All input images are resized to a unified resolution of 384×384 . The per-device batch

TABLE II

MAIN EVALUATION RESULTS ON MUSON DATASET. WE PRESENT A COMPREHENSIVE QUANTITATIVE EVALUATION ACROSS THREE DIMENSIONS: DECISION PRECISION, SAFETY COMPLIANCE, AND REASONING QUALITY. NOTE THAT QWEN2.5-VL-3B DEMONSTRATES SUPERIOR PERFORMANCE ACROSS ALL METRICS, ESTABLISHING A STRONG BASELINE FOR THE TASK.

Model	Decision Precision		Safety	Reasoning Quality (S_{bert}) ↑			
	Acc. ↑	Macro-F1 ↑	CR ↓	Perception	Prediction	Reasoning	Explanation
TinyLLaVA (Phi-2)	0.6062	0.3402	0.2063	0.7471	0.7408	0.7870	0.8023
NVILA	0.1761	0.1575	0.4813	0.6817	0.6842	0.7436	0.7522
Qwen2.5-VL-3B	0.8625	0.7706	0.0688	0.8809	0.8768	0.8729	0.8868
MoE-LLaVA	0.5813	0.2908	0.1313	0.7625	0.7566	0.7919	0.8124

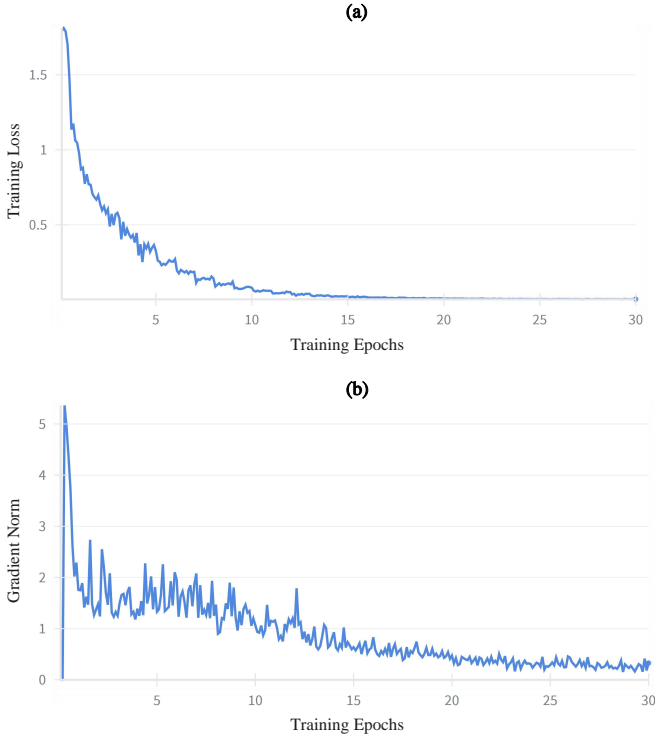


Fig. 3. **Training loss and gradient norm curves.** (a) Fine-tuning loss curve of TinyLLaVA on MUSON. (b) Corresponding gradient norm curve.

size is 4, resulting in a global batch size of 32 across all GPUs. Training is conducted for a total of 30 epochs to ensure adequate learning of rare samples under the long-tailed data distribution.

B. Main Evaluations

Comparative Analysis of SVLM Baselines. As shown in Table II, different SVLM architectures exhibit distinct navigation behaviors when trained on MUSON. Qwen2.5-VL-3B achieves the strongest overall fitting performance. In contrast, the weaker performance of NVILA suggests that short-horizon social reasoning requires not only high-quality data but also appropriate architectural compatibility. Fig. 4 presents qualitative visualizations of high-level action decisions, while Fig. 5 illustrates high-level semantic reasoning quality.

Reasoning Quality and Semantic Alignment. As shown in Table II, semantic alignment consistently improves from

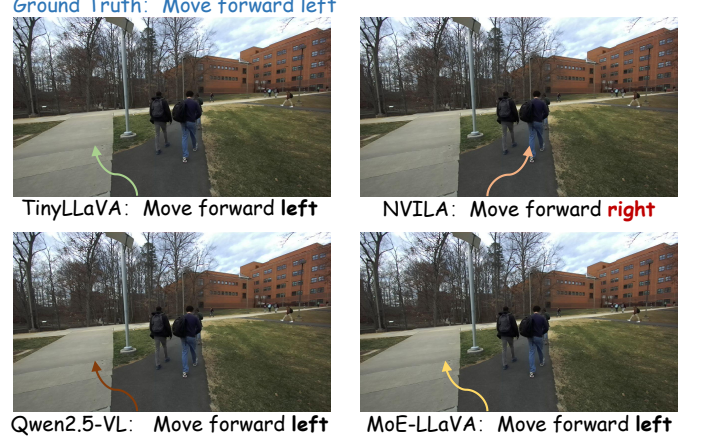


Fig. 4. **Visualization of high-level decision results for different SVLMs on MUSON.**

TABLE III
IMPACT OF CoT QUALITY ON DECISION ACCURACY. QUANTITATIVE COMPARISON WITH MOE-LLAVA UNDER ACTION-ONLY AND FIVE-TURN CONVERSATION SETTINGS. FIVE-TURN TRAINING IMPROVES ACCURACY ON MUSON BUT DEGRADES PERFORMANCE ON SNEI, LIKELY DUE TO INCONSISTENT REASONING, ACTIONS, AND EXPLANATIONS IN SNEI DATASET.

Configuration	Acc. ↑	
	SNEI	MUSON (Ours)
Action Only	0.5833	0.5375
With CoT	0.4667	0.5813

perception to explanation, indicating increasing reasoning consistency toward final decision making. In particular, the high score at the *Explanation* stage (0.8868 for Qwen2.5-VL-3B) suggests that the model captures meaningful retrospective rationales from MUSON rather than merely reflecting low-level visual descriptions.

Efficacy of CoT and Dataset Validation. To validate the quality of MUSON and its CoT annotations, we compare MoE-LLaVA performance on SNEI and MUSON under *Action-Only* and *CoT* settings (Table III). The results highlight the decisive role of data quality in enabling effective reasoning for SVLMs.

On SNEI, incorporating CoT leads to a substantial accuracy drop (0.5833 → 0.4667), indicating that its inconsistent reasoning-action alignment introduces noise rather than use-

 Ground Truth	Perception: Two pedestrians are in front on the sidewalk, both moving to the right. The background has a brick building, a bus stop, and static objects like a parked car and street signs. Prediction: The two pedestrians will continue walking to the right, away from the robot's direct path. The building, bus stop, car, and street signs remain static. Reasoning: Since the pedestrians are moving to the right and the background objects are static, the robot needs to continue straight without adjustment. Action: Move forward Explanation: I see two pedestrians crossing to the right in front of me, and static objects like the building and bus stop. I will move straight at normal speed because the path ahead is clear.		
	TinyLLaVA (Phi2)	NVILA	Qwen2.5-VL-3B
Perception: A person in black clothes is walking backward ahead, and a crowd is walking forward in the far distance ahead.	Perception: A crowd is walking forward in the far distance ahead.	Perception: Two pedestrians are directly ahead on the sidewalk, both walking toward the right side. The background features a brick building, a bus stop, and several parked vehicles.	Perception: One pedestrian is on the crosswalk to the right, walking across the road from left to right. The background includes a brick building, bushes, a bus stop, and a parking structure.
Prediction: The person in black ahead will continue walking backward, and the crowd in the far distance ahead will continue walking forward.	Prediction: The crowd in the far distance ahead will continue walking forward.	Prediction: The two pedestrians will continue moving to the right across the sidewalk, temporarily blocking the robot's forward path.	Prediction: The pedestrian will keep moving to the right side across the crosswalk. The building, bushes, bus stop, and parking structure will remain static.
Reasoning:	Reasoning:	Reasoning:	Reasoning:
Action: Move forward	Action: Move forward right	Action: Turn right	Action: Move forward
Explanation:	Explanation:	Explanation:	Explanation:

Fig. 5. Visualization of high-level reasoning quality for different SVLMs on MUSON.

ful supervision. In contrast, on MUSON, CoT consistently improves performance ($0.5375 \rightarrow 0.5813$), demonstrating that well-structured and logically consistent annotations allow CoT to function as an effective reasoning scaffold. These results confirm that MUSON provides reliable supervision for reasoning-oriented navigation, whereas poorly aligned CoT annotations can be detrimental to capacity-limited SVLMs.

C. Limitations and Future Work

While this work represents a meaningful step forward, several limitations point to promising directions for future research.

Data-level. Rather than focusing solely on dataset scale, future work will investigate how structured annotations can more efficiently convey high-value supervisory signals under limited data budgets. In particular, we aim to refine annotation granularity and supervision design to identify which elements, such as social cues, spatial constraints, or causal rationales, most effectively enhance embodied reasoning and generalization.

Model-level. Beyond supervised fine-tuning, we plan to explore benchmark-driven optimization of SVLMs by leveraging MUSON's structured CoT annotations. Integrating reinforcement learning and continual adaptation mechanisms is a key direction to better align reasoning with sequential decision-making in dynamic environments, especially for lightweight models deployed under real-world constraints.

VI. CONCLUSION

This paper makes two primary contributions: the introduction of a high-quality dataset and a systematic benchmark for socially compliant navigation. First, we present MUSON, a multimodal dataset for short-horizon social navigation, featuring structured five-step Chain-of-Thought annotations and a rational, de-biased action distribution. Second, we benchmark state-of-the-art SVLMs on MUSON to evaluate safety (CR), semantic reasoning consistency (SBERTScore), and decision accuracy (Acc., Macro-F1). Experimental results show that Qwen2.5-VL-3B achieves the best high-level decision accuracy and semantic reasoning performance, and that, with MUSON supervision, even lightweight models can learn meaningful and safe navigation policies and generalize effectively across diverse real-world scenarios.

REFERENCES

- [1] P. Anderson, Q. Wu, D. Teney, J. Bruce, M. Johnson, N. Sünderhauf, I. Reid, S. Gould, and A. Van Den Hengel, "Vision-and-language navigation: Interpreting visually-grounded navigation instructions in real environments," in *Proceedings of the IEEE Conference on Computer Vision and Pattern Recognition (CVPR)*, 2018, pp. 3674–3683.
- [2] A. Ku, P. Anderson, R. Patel, E. Ie, and J. Baldridge, "Room-across-room: Multilingual vision-and-language navigation with dense spatiotemporal grounding," in *Proceedings of the Conference on Empirical Methods in Natural Language Processing (EMNLP)*, 2020, pp. 4379–4412.
- [3] A. J. Sathyamoorthy, K. Weerakoon, M. Elnoor, A. Zore, B. Ichter, F. Xia, J. Tan, W. Yu, and D. Manocha, "Convoi: Context-aware navigation using vision language models in outdoor and indoor environments," in *Proceedings of the IEEE/RSJ International Conference on Intelligent Robots and Systems (IROS)*, 2024, pp. 13 837–13 844.

[4] S. Luo, P. Sun, J. Zhu, Y. Deng, C. Yu, A. Xiao, and X. Wang, “Gson: A group-based social navigation framework with large multimodal model,” *IEEE Robotics and Automation Letters*, 2025.

[5] T. Kawabata, X. Zhang, and L. Xiao, “Socialnav-moe: A mixture-of-experts vision language model for socially compliant navigation with reinforcement fine-tuning,” *arXiv preprint arXiv:2512.14757*, 2025.

[6] A. Payandeh, D. Song, M. Nazeri, J. Liang, P. Mukherjee, A. H. Raj, Y. Kong, D. Manocha, and X. Xiao, “Social-llava: Enhancing robot navigation through human-language reasoning in social spaces,” *arXiv preprint arXiv:2501.09024*, 2024.

[7] J. Krantz, E. Wijmans, A. Majumdar, D. Batra, and S. Lee, “Beyond the nav-graph: Vision-and-language navigation in continuous environments,” in *Proceedings of the European Conference on Computer Vision (ECCV)*, 2020.

[8] D. Shah, A. Sridhar, A. Bhorkar, N. Hirose, and S. Levine, “Gnm: A general navigation model to drive any robot,” in *Proceedings of the IEEE International Conference on Robotics and Automation (ICRA)*, 2023, pp. 7226–7233.

[9] J. Zhang, K. Wang, R. Xu, G. Zhou, Y. Hong, X. Fang, Q. Wu, Z. Zhang, and H. Wang, “Navid: Video-based vlm plans the next step for vision-and-language navigation,” *arXiv preprint arXiv:2402.15852*, 2024.

[10] R. Martin-Martin, M. Patel, H. Rezatofighi, A. Shenoj, J. Gwak, E. Frankel, A. Sadeghian, and S. Savarese, “Jrdb: A dataset and benchmark of egocentric robot visual perception of humans in built environments,” *IEEE Transactions on Pattern Analysis and Machine Intelligence*, vol. 45, no. 6, pp. 6748–6765, 2021.

[11] H. Karnan, A. Nair, X. Xiao, G. Warnell, S. Pirk, A. Toshev, J. Hart, J. Biswas, and P. Stone, “Socially compliant navigation dataset (scand): A large-scale dataset of demonstrations for social navigation,” *IEEE Robotics and Automation Letters*, vol. 7, no. 4, pp. 11 807–11 814, 2022.

[12] F. Codevilla, M. Müller, A. López, V. Koltun, and A. Dosovitskiy, “End-to-end driving via conditional imitation learning,” in *Proceedings of the IEEE International Conference on Robotics and Automation (ICRA)*, 2018, pp. 4693–4700.

[13] M. Bansal, A. Krizhevsky, and A. Ogale, “Chauffeurnet: Learning to drive by imitating the best and synthesizing the worst,” *arXiv preprint arXiv:1812.03079*, 2018.

[14] F. Codevilla, E. Santana, A. M. López, and A. Gaidon, “Exploring the limitations of behavior cloning for autonomous driving,” in *Proceedings of the IEEE/CVF International Conference on Computer Vision (ICCV)*, 2019, pp. 9329–9338.

[15] D. Driess, F. Xia, M. S. Sajjadi, C. Lynch, A. Chowdhery, B. Ichter, A. Wahid, J. Tompson, Q. Vuong, T. Yu *et al.*, “Palm-e: an embodied multimodal language model,” in *Proceedings of the 40th International Conference on Machine Learning (ICML)*, 2023, pp. 8469–8488.

[16] B. Zitkovich, T. Yu, S. Xu, P. Xu, T. Xiao, F. Xia, J. Wu, P. Wohlhart, S. Welker, A. Wahid *et al.*, “Rt-2: Vision-language-action models transfer web knowledge to robotic control,” in *Proceedings of the Conference on Robot Learning (CoRL)*, 2023, pp. 2165–2183.

[17] W. Huang, P. Abbeel, D. Pathak, and I. Mordatch, “Inner monologue: Embodied reasoning through planning with language models,” in *Proceedings of the Conference on Robot Learning (CoRL)*, 2022, pp. 1769–1782.

[18] S. Yao, J. Zhao, D. Yu, N. Du, I. Shafran, K. R. Narasimhan, and Y. Cao, “React: Synergizing reasoning and acting in language models,” in *Proceedings of the 11th International Conference on Learning Representations (ICLR)*, 2022.

[19] W. Huang, C. Wang, R. Zhang, Y. Li, J. Wu, and L. Fei-Fei, “Voxposer: Composable 3d value maps for robotic manipulation with language models,” in *Proceedings of the Conference on Robot Learning (CoRL)*, 2023, pp. 540–562.

[20] S. Vemprala, R. Bonatti, A. Bucker, and A. Kapoor, “Chatgpt for robotics: Design principles and model abilities,” *IEEE Access*, vol. 12, pp. 5565–5578, 2024.

[21] N. Wake, A. Kanehira, K. Sasabuchi, J. Takamatsu, and K. Ikeuchi, “Chatgpt empowered long-step robot control in various environments: A case application,” in *Proceedings of the IEEE/RSJ International Conference on Intelligent Robots and Systems (IROS)*, 2023, pp. 86–93.

[22] L. Xiao and T. Yamasaki, “Llm-advisor: An llm benchmark for cost-efficient path planning across multiple terrains,” *arXiv preprint arXiv:2503.01236*, 2025.

[23] P. Zhang, G. Zeng, T. Wang, and W. Lu, “Tinyllama: An open-source small language model,” *arXiv preprint arXiv:2401.02385*, 2024.

[24] X. Chu, L. Qiao, X. Lin, S. Xu, Y. Yang, Y. Hu, F. Wei, X. Zhang, B. Zhang, X. Wei *et al.*, “Mobilevlm: A fast, strong and open vision language assistant for mobile devices,” *arXiv preprint arXiv:2312.16886*, 2023.

[25] B. Zhou, Y. Hu, X. Weng, J. Jia, J. Luo, X. Liu, J. Wu, and L. Huang, “Tinyllava: A framework of small-scale large multimodal models,” *arXiv preprint arXiv:2402.14289*, 2024.

[26] B. Lin, Z. Tang, Y. Ye, J. Cui, B. Zhu, P. Jin, J. Huang, J. Zhang, Y. Pang, M. Ning *et al.*, “Moe-llava: Mixture of experts for large vision-language models,” *arXiv preprint arXiv:2401.15947*, 2024.

[27] J. Bai, S. Bai, Y. Chu, Z. Cui, K. Dang, X. Deng, Y. Fan, W. Ge, Y. Han, F. Huang *et al.*, “Qwen technical report,” *arXiv preprint arXiv:2309.16609*, 2023.

[28] J. Wei, X. Wang, D. Schuurmans, M. Bosma, F. Xia, E. Chi, Q. V. Le, D. Zhou *et al.*, “Chain-of-thought prompting elicits reasoning in large language models,” in *Proceedings of the Advances in neural information processing systems (NeurIPS)*, vol. 35, 2022, pp. 24 824–24 837.

[29] D. M. Nguyen, M. Nazeri, A. Payandeh, A. Datar, and X. Xiao, “Toward human-like social robot navigation: A large-scale, multi-modal, social human navigation dataset,” in *Proceedings of the IEEE/RSJ International Conference on Intelligent Robots and Systems (IROS)*, 2023, pp. 7442–7447.

[30] H. Seong, S. Kim, M. Kim, Y. Cho, M. Joe, S. Choi, J. Jung, J. Youn, Y. Kim, S. Seong *et al.*, “Costnav: A navigation benchmark for cost-aware evaluation of embodied agents,” *arXiv preprint arXiv:2511.20216*, 2025.

[31] K. Papineni, S. Roukos, T. Ward, and W.-J. Zhu, “Bleu: a method for automatic evaluation of machine translation,” in *Proceedings of the 40th annual meeting of the Association for Computational Linguistics (ACL)*, 2002, pp. 311–318.

[32] N. Reimers and I. Gurevych, “Sentence-bert: Sentence embeddings using siamese bert-networks,” in *Proceedings of the Conference on Empirical Methods in Natural Language Processing and the 9th International Joint Conference on Natural Language Processing (EMNLP-IJCNLP)*, 2019, pp. 3982–3992.

[33] Z. Liu, L. Zhu, B. Shi, Z. Zhang, Y. Lou, S. Yang, H. Xi, S. Cao, Y. Gu, D. Li *et al.*, “Nvila: Efficient frontier visual language models,” in *Proceedings of the Computer Vision and Pattern Recognition Conference (CVPR)*, 2025, pp. 4122–4134.

[34] S. Bai, K. Chen, X. Liu, J. Wang, W. Ge, S. Song, K. Dang, P. Wang, S. Wang, J. Tang *et al.*, “Qwen2. 5-vl technical report,” *arXiv preprint arXiv:2502.13923*, 2025.